

A New Candidate Active Antenna Design for the Long Wavelength Array

Nagini Paravastu (ASEE/NRL), Brian Hicks (NRL)

Paul Ray (NRL), William Erickson (UMD)

May 2, 2007

Abstract

This report introduces a new antenna design - the fork antenna - that is intended to be an alternative to the baseline big blade design in the LWA project. The fork antenna is a simpler design than the big blade, and could cost significantly less. Simulation results and field measurements are presented to show that the fork antenna performs comparably to the big blade. The fork antenna could therefore be an attractive alternative to the big blade antenna.

I. INTRODUCTION

The Long Wavelength Array (LWA), currently in the development stage, is a radio telescope array that will be constructed in New Mexico, USA over the next several years [1]. It will consist of ~ 52 stations of ~ 256 cross-dipole antennas each, and will explore the Universe in the 20 – 80 MHz frequency band. The large number of antennas required for the LWA suggests that the antenna design must be kept simple in order to maintain a low station cost. The leading candidate LWA antenna is a “big blade” antenna consisting of crossed dipole elements made of sheet aluminum [2]. The big blade antenna has been extensively characterized and shows potential for fulfilling the technical requirements for the LWA. However, the potentially prohibitive cost has necessitated the exploration of alternate, more affordable antenna topologies. In this paper, we present one such promising topology – the fork antenna. In the following sections, we show through simulation and field measurement that the fork antenna compares closely in performance to the big blade antenna and could therefore be a practical alternative to the big blade antenna for the LWA project.

II. DESCRIPTION OF TOPOLOGY

Figure 1 shows a drawing of the fork antenna (left), and a drawing of the big blade is also shown in Figure 1 (right) for comparison. The fork antenna, like the big blade, is a dipole-like structure, but it is a simpler design. The radiating elements on the big blade antenna are made of sheet aluminum, which is one of its major cost drivers. The fork antenna topology eliminates the need for sheet metal and instead uses three strands of wire or cable to simulate the skeletal outline of a blade. The fork antenna is also less susceptible to wind loading than the big blade antenna, which is a major concern in the New Mexico desert. Additionally, the support structure required for the fork antenna will likely be less intricate than that which will be required for the big blade antenna. Although manufacturing cost estimates have not yet been completed, the fork antenna could be less expensive than the big blade antenna.

III. SIMULATION

The characteristics of the fork antenna were simulated using NEC-4, and compared to previous simulations of the big blade antenna. Earth ground conditions ($\epsilon_r = 13, \sigma = 0.005S/m$) were assumed for all simulations. For simplicity, the wires in the antenna elements were assumed to be perfect conductors since metal losses are negligible at these frequencies. Each arm of the fork antenna consists of three 1.5 m long wires evenly distributed over a 30° flare angle. The feed point stands 1.5 m above the ground and

each radiating element is drooped 45° below horizontal. The elements in the big blade antenna are 1.7 m long, 42 cm wide, and are drooped 45° below horizontal.

Figure 2 shows the simulated impedances of the big blade and fork antennas. The spike at 64 MHz is believed to be a simulation artifact and not a real physical effect. The fork antenna has a higher resonant frequency than the blade, but this can easily be changed if necessary by adjusting the lengths of the radiating elements. Figure 3 shows the calculated impedance mismatch efficiency (IME) for a 100Ω load. The IME is given by $1 - \Gamma^2$ where Γ is the simulated reflection coefficient at the antenna feed point. The IME curve of the two antennas show the same basic properties with the fork antenna curve being $\sim 1 - 2$ dB lower across the simulated frequency range.

Figure 4 shows the computed E – and H – plane beam patterns of the two antennas at 38 MHz and 74 MHz. The fork and big blade antennas exhibit similar beam characteristics at both frequencies. Figure 5 shows the calculated Galactic power density at the antenna feed point (preamplifier input) for the fork and big blade antennas. These calculations were based on the Cane Galactic temperature model and the methods given by S. Ellingson and A. Kerkhoff in [3] and [4]. The power density resulting from the Hicks balun (with a noise temperature of 250 K) is also shown for comparison. Simulation results show that both antennas, paired with a 250 K noise temperature preamplifier, exhibit the required Galactic noise dominated performance over the 20 – 80 MHz LWA frequency band. The fork antenna shows a slight improvement in detected power density over the blade antenna at higher frequencies, but a slight degradation at lower frequencies. Overall, the simulated behavior of the fork antenna was found to be comparable to the big blade antenna.

IV. PROTOTYPE CONSTRUCTION

Once the fork antenna had been characterized through simulation, a prototype was constructed for field testing. For simplicity, a single polarization prototype was constructed, but a dual polarization version of this antenna will likely have nearly identical characteristics. Three strands of 25/32" diameter tinned copper tubular braid from Jaguar Industries, Inc. (part number JTTB-176) were welded together at one end to form the fork antenna radiating elements [5]. The welded ends were then mated to a Hicks balun. The prototype was mounted to a PVC mast and the free ends of the braided cables were anchored to the ground with twine and tent stakes. A photograph of the fork antenna prototype is shown in Figure 6 and a picture of the big blade antenna is shown in Figure 7 for comparison.

V. FIELD MEASUREMENTS

The objective of the field test, performed in November 2006, was to collect sky noise data and compare the detected power levels to predictions based on NEC-4 simulations. The fork antenna prototype was deployed at the Very Large Array site in New Mexico, where spectra were recorded over a 24 hour period. The preamplifier used in these measurements was the Hicks balun [6].

A diagram of the antenna measurement system is shown in Figure 8. The signals were transmitted from the Fork antenna/Hicks balun to the Specmaster RFI monitoring system over 88 ft (26.8 m) of RG-58 coaxial cable [7]. A bias-T was used to separate the received RF signal from the DC power being supplied to the Hicks balun over the same coaxial cable. A *Minicircuits* ZHL-1A 16 dB amplifier was also used to amplify detected signals to power levels that were well over the noise floor of the spectrum analyzer. Table I shows the noise temperature, noise figure and gain of each component in the measurement chain. The total system noise temperature, noise figure and gain are also shown in Table I, and were calculated using a Friis cascade analysis of the measurement system.

Figure 9 shows one sample measured spectrum. HF communication signals, audio and video carriers for local television channels 2, 4, and 5, as well as FM radio signals can be seen in all of the recorded spectra. In between, there are windows with little or no pollution from terrestrial signals that can be used for radio astronomy observations. The power level variation in the noise floor is the result of the frequency dependent coupling of the Galactic background noise power into the antenna. The dashed

curve represents the predicted detected power levels, which were calculated using the Cane Galactic noise temperature model, NEC-4 simulation data on the fork antenna. This calculation also includes the total system noise and gain contributions given in Table I. The basic equations used are given here.

The observed antenna temperature at the preamplifier input is given by

$$T_{ant} = \epsilon_r(1 - |\Gamma|^2)T_{sky}, \quad (1)$$

where ϵ_r is the simulated ground loss factor, Γ is the simulated antenna reflection coefficient, and T_{sky} is the Galactic noise temperature derived from the Cane model. The total noise temperature detected at the spectrum analyzer input is given by

$$T_{tot} = T_{ant} + T_{receiver}, \quad (2)$$

where $T_{receiver}$ is the total system noise temperature given in Table I. Finally, the total power detected by the spectrum analyzer is given by

$$P_{tot} = kT_{tot}B + G_{receiver}, \quad (3)$$

where k is Boltzmann's constant, B is the resolution bandwidth used in the measurement (51 kHz) and $G_{receiver}$ is the total system gain given in Table I. The offset between simulation and measurement is likely due to the use of manufacturer specified gain/loss and noise figures for the components in the measurement system in the Friis analysis instead of values directly measured using a network analyzer.

The smooth curve in Figure 9, added for comparison, shows the simulated detected power for an antenna that is perfectly impedance matched to the sky (i.e., $\Gamma = 0$ and $\epsilon_r = 0$).

Figure 10 shows a plot of detected power over a 24 hour period for six different frequencies ranging from 33 MHz to 110 MHz for both the big blade antenna and fork antenna. As time passes, the detected power levels at these frequencies increase and decrease with the period of the rising and setting of the Galactic Center in the sky. This indicates that the fork antenna/Hicks balun and big blade/Hicks balun systems are Galactic noise dominated. However, the amplitudes of these curves decrease with increasing frequency, indicating that Galactic noise dominance is decreasing at higher frequencies for both antennas. The measurement results for the two antennas are comparable, but the irregularities in the fork antenna curves at higher frequencies are of some concern and could be due to beam pattern degradation at those frequencies. In the near future, additional measurements will be performed on the fork antenna and Hicks balun at the LWDA site in an effort to understand previous observations. These observations will be presented in future LWA memos.

VI. SUMMARY

We have presented simulation and field measurements on a new candidate antenna design for the LWA. Simulations show that the fork antenna, paired with the Hicks balun (with a noise temperature of 250 K) exhibits Galactic noise dominated performance over the the 20 – 80 MHz LWA band. Furthermore, the simulated sky noise dominance of the fork antenna appears comparable to the big blade antenna.

Further investigation of the fork antenna is needed to bring the fork antenna design to the level of confidence of the big blade antenna. Both the big blade and fork antenna designs have gone through only a minimal level of optimization. In the future, a complete parametric optimization will be done on both antennas. Additional Galactic noise measurements must also be taken of the fork antenna prototype to supplement the first 24 hours of data obtained in November of 2006. The behavior of these antennas in an array configuration must be considered as well since mutual coupling between antennas in close proximity may have a significant impact on antenna characteristics which could in turn affect station beam properties. In addition, efforts are already underway to obtain cost estimates for both antennas. These studies will provide the information necessary to properly understand the cost-performance tradeoffs between the two antennas.

TABLE I
NOISE TEMPERATURE, NOISE FIGURE AND GAIN OF COMPONENTS IN MEASUREMENT SYSTEM

	Noise Temperature (K)	Noise Figure (dB)	Gain (dB)
Hicks balun (10 – 100 MHz)	250	2.7	24
RG-58 coax cable (10 – 100 MHz)	150 – 750	1.8 – 5.5	-1.8 – -5.5
Bias-T (10 – 100 MHz)	35	0.5	-0.5
Minicircuits ZHL-1A amplifier (10 – 100 MHz)	3360	11	16
Total System (10 – 100 MHz)	275 – 310	2.9 – 3.2	37.5 – 33.8

ACKNOWLEDGMENTS

Basic research in radio astronomy at the Naval Research Laboratory is supported by 6.1 base funding. The authors are grateful to Dr. Kenneth Stewart of the Naval Research Laboratory and Dr. Steven Ellingson of Virginia Tech for their assistance with the antenna simulations.

REFERENCES

- [1] "LWA: The Long Wavelength Array," <http://lwa.unm.edu/>, 2004.
- [2] W. Erickson, "Tests on Large Blade Dipoles," *LWA Memo Series (Memo 36)*, May 2006.
- [3] H. Cane, "Spectra of the Nonthermal Radio Radiation from the Galactic Polar Regions," *Monthly Notice Royal Astronomical Society*, vol. 189, p. 465, 1979.
- [4] S. Ellingson and A. Kerkhoff, "Comparison of Two Candidate Elements for a 30-90 MHz Radio Telescope Array," *2005 IEEE International Antennas and Propagation Society Symposium*, vol. 1A, pp. 590–593, July 2004.
- [5] "Jaguar Industries, Inc.," <http://www.jaguarind.com/products/busbarbraid/tubular.html>.
- [6] R. Bradley and C. Parashare, "Evaluation of the NRL LWA Active Balun Prototype (Rev.A)," *LWA Memo Series (Memo 19)*, February 2005.
- [7] B. Hicks, P. Ray, N. Paravastu, R. Duffin, and S. Ellingson, "Specmaster: A Simple Spectrum Monitoring Tool," *LWA Memo Series (Memo 74)*, January 2007.

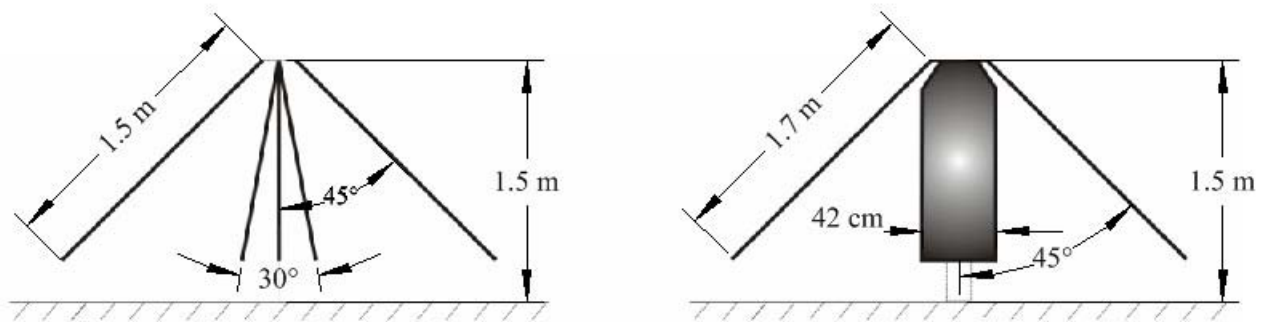


Fig. 1. Drawings of the fork antenna (left) and the big blade antenna (right).

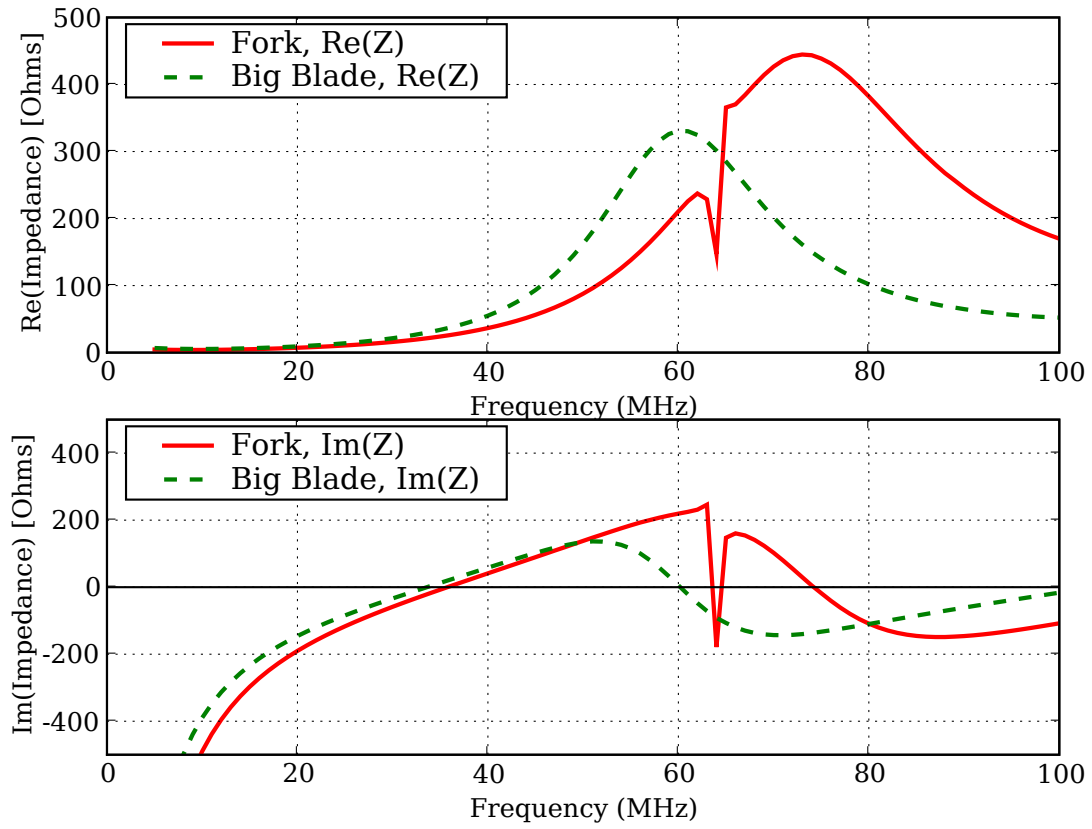


Fig. 2. Big blade and fork antenna impedances simulated using *NEC-4*.

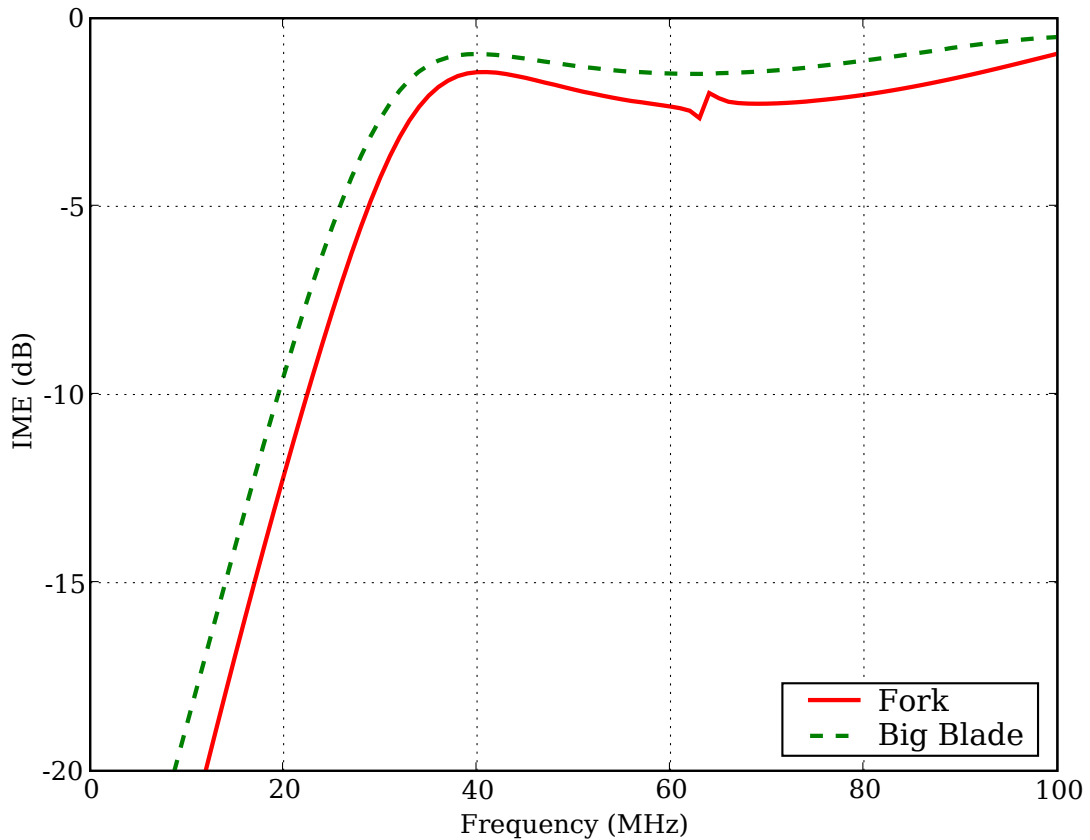


Fig. 3. Calculated impedance mismatch efficiency for a 100Ω load (based on *NEC-4* simulation results).

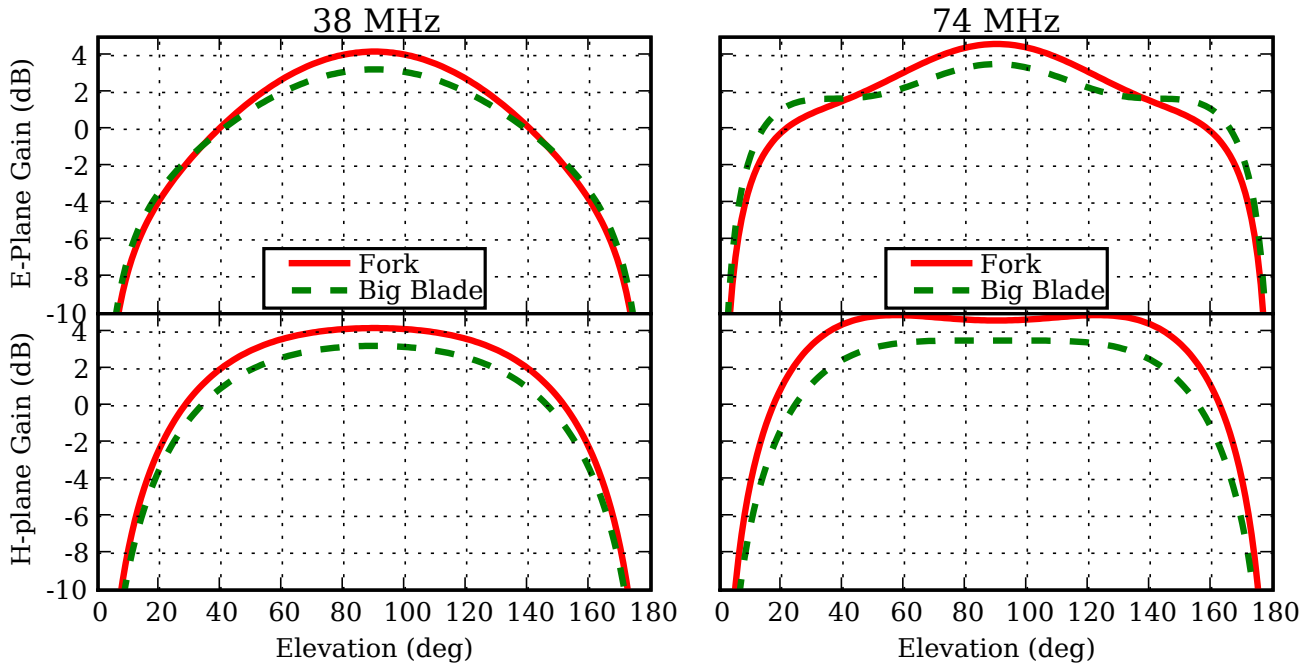


Fig. 4. Simulated beam patterns of the fork and big blade antennas at 38 MHz (left) and 74 MHz (right). Zenith = 90° .

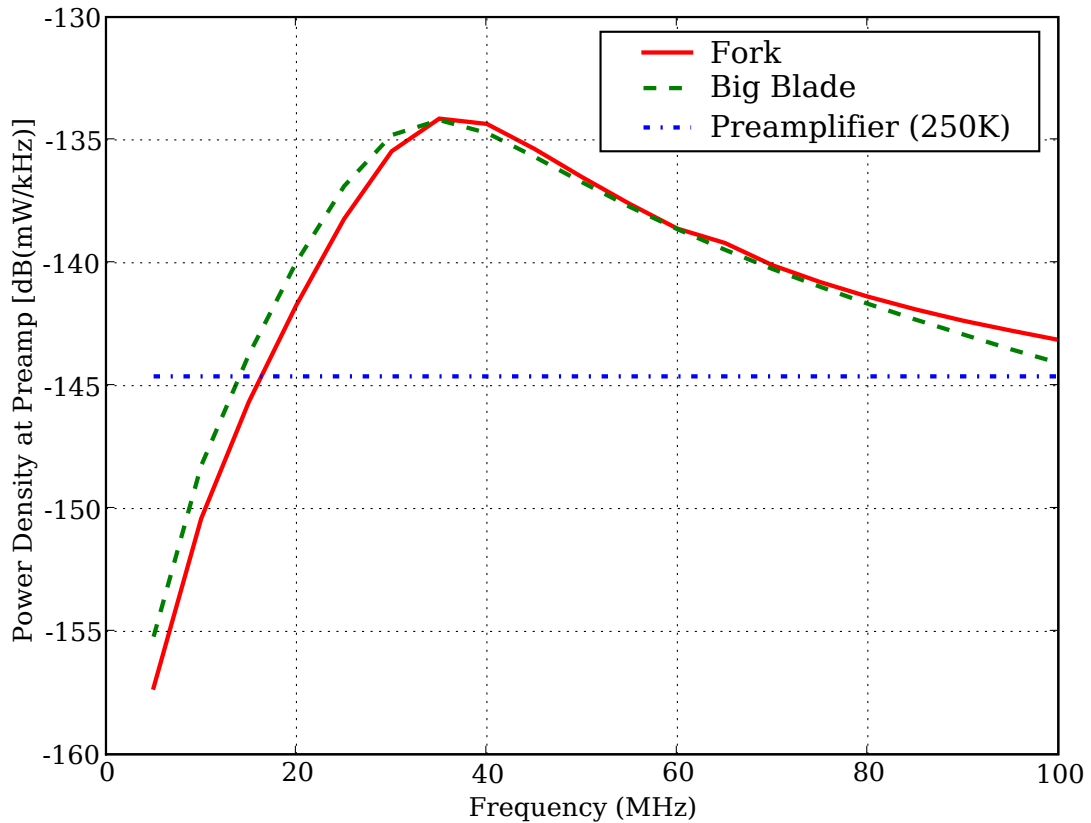


Fig. 5. The simulated Galactic noise power density at the antenna feed point (preamplifier input) for the fork antenna and the big blade antenna. The power density generated by a preamplifier with a noise temperature of 250 K is also shown. When the Galactic power density at the antenna feed point is greater than that of the preamplifier, the antenna is said to be operating with Galactic noise dominated performance.

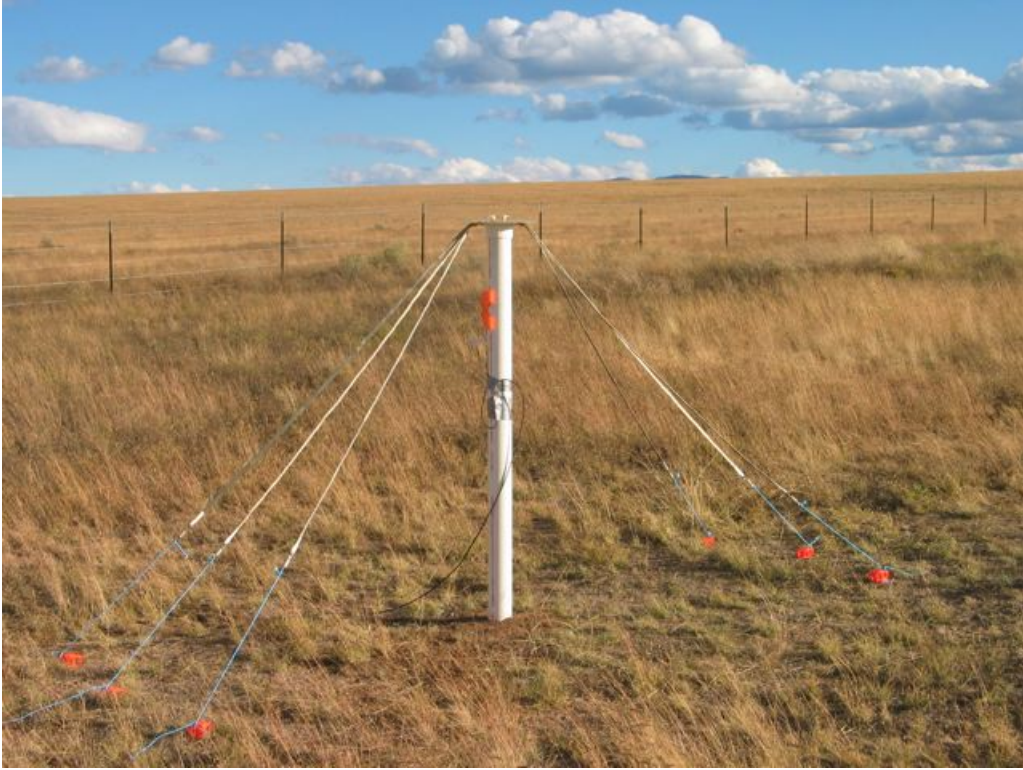


Fig. 6. A photograph of the single polarization fork antenna prototype, currently deployed at the LWDA site.



Fig. 7. A photograph of the dual polarization big blade antenna prototype (right), currently deployed at the LWDA site.

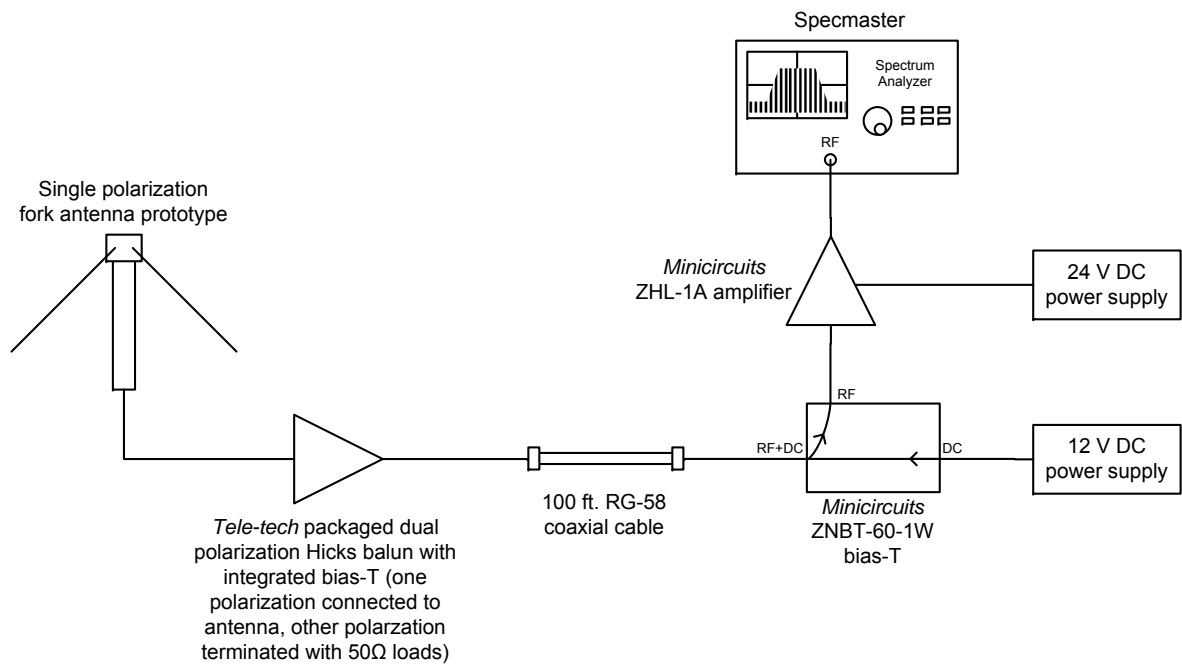


Fig. 8. A diagram of the fork antenna sky noise measurement system.

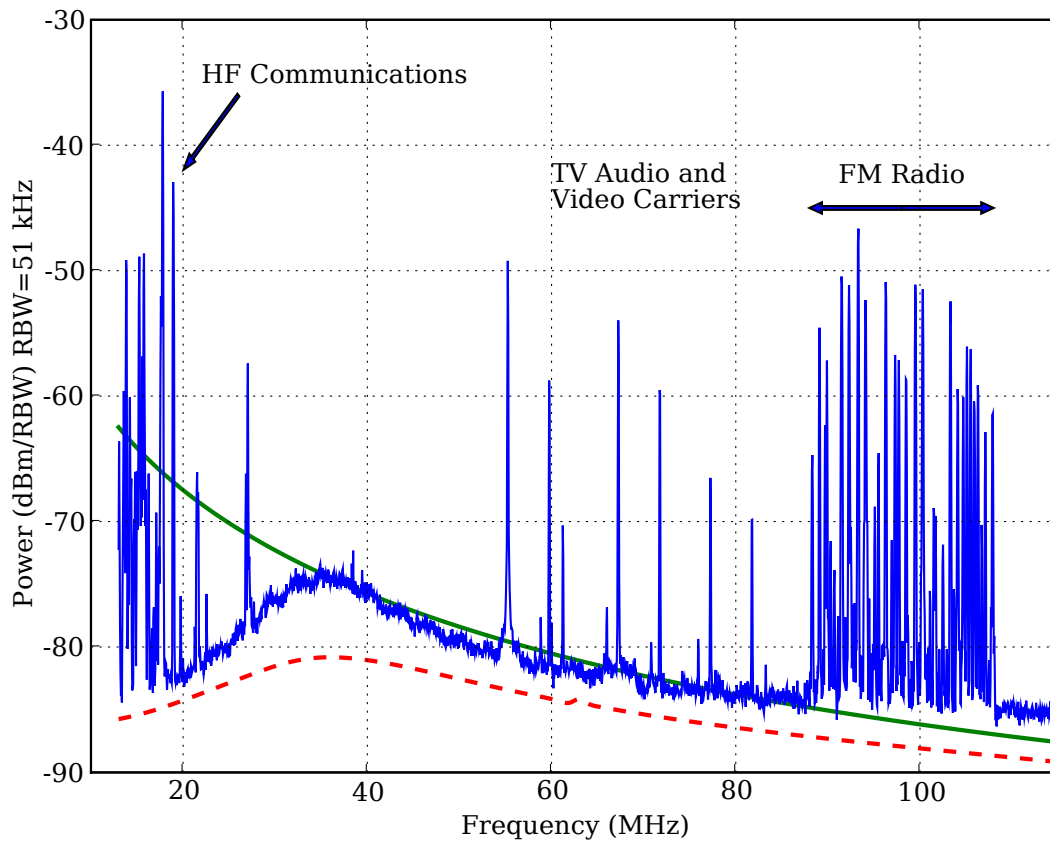


Fig. 9. A spectrum recorded with the fork antenna at the Very Large Array site in New Mexico. The dashed curve is a theoretical prediction of the detected power based on NEC-4 simulations of the fork antenna and the Cane Galactic noise temperature model. Simulated ground loss, measurement system gain, and measurement system noise temperature (calculated using a Friis cascade analysis of the system) are also reflected in this curve. The smooth curve, added for comparison, is a prediction of the detected power for an antenna that is perfectly impedance matched to the sky and with no ground losses (i.e., $\Gamma = 0$ and $\epsilon_r = 0$).

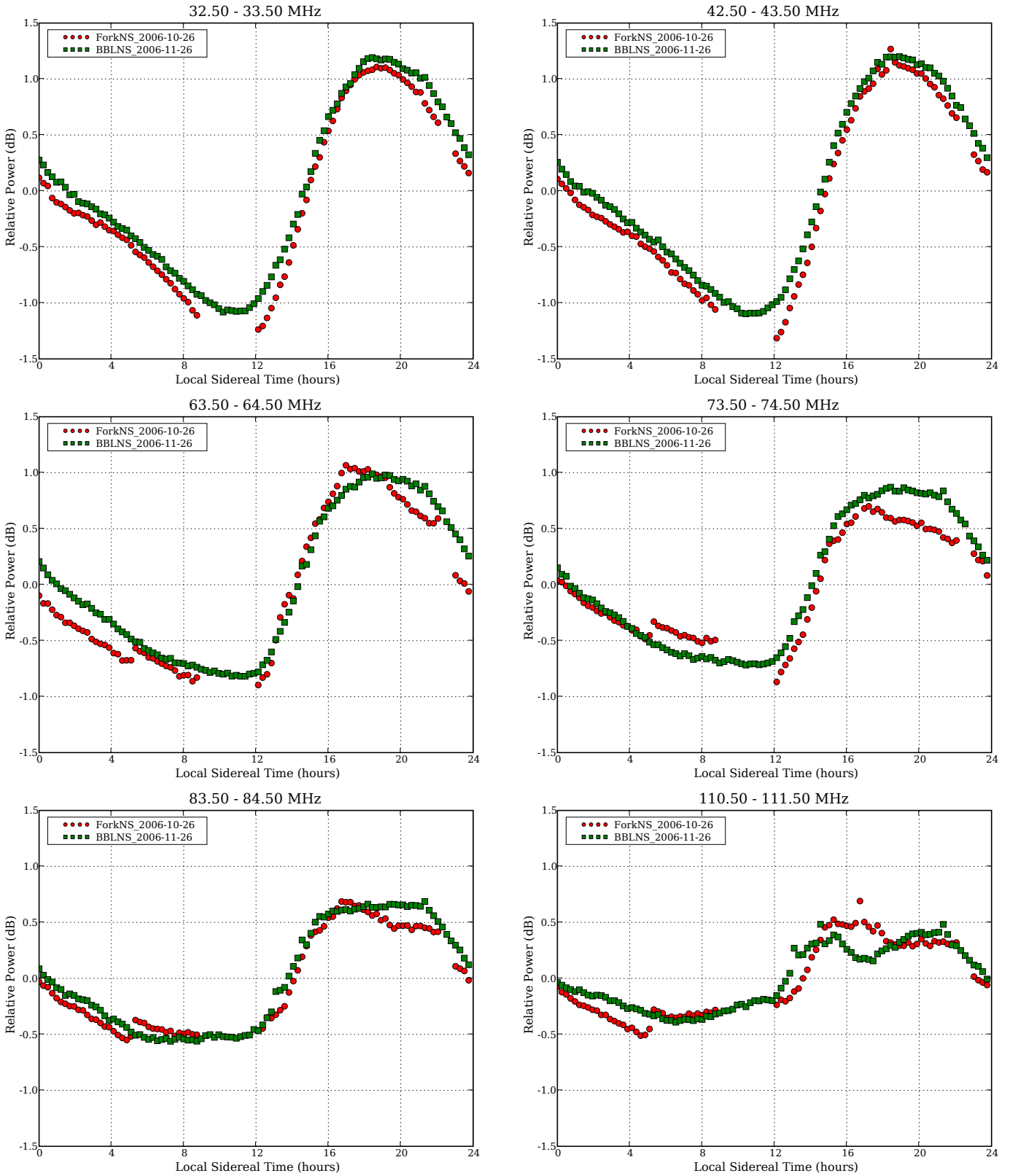


Fig. 10. Plots of power detected by the fork and big blade antennas as a function of time. Gaps in the fork antenna data are the result of times when the spectrum monitoring system was briefly deactivated. The legend label ForkNS_2006-10-26 indicates that the fork antenna data were taken on October 26, 2006 with the antenna oriented north-south. Similarly, BBLNS_2006-11-26 indicates that the big blade data were taken on November 26, 2006 with the antenna oriented north-south.